Journal of Inclusion Phenomena and Macrocyclic Chemistry (2022) 102:763–780
https://doi.org/10.1007/s10847-022-01157-y

ORIGINAL ARTICLE

Synthesis, antimicrobial and thermal studies of nitropyridine-substituted double armed benzo-15-crown-5 ligands; alkali (Na^+ and K^+) and transition metal (Ag^+) complexes; reduction of nitro compounds

Serhat Koçoğlu[1,2] · Zeliha Hayvali[2] · Hatice Ogutcu[3] · Orhan Atakol[2]

Received: 17 May 2022 / Accepted: 3 August 2022 / Published online: 26 August 2022

Abstract

Nitropyridine substituted double-armed benzo 15-crown-5 compounds (**1–4**) were synthesized by the reactions of 4′,5′-bis(bromomethyl)benzo-15-crown-5 with hydroxypyridine derivatives. Na^+ and K^+ complexes (**1a–4a, 1b–4b**) of crown ether compounds (**1–4**) were prepared with sodium picrate and potassium picrate, respectively. Transition metal complexes (**1c–4c**) of the synthesized ligands (**1–4**) were prepared from Ag^+ cation. In addition, nitro compounds (**1, 2** and **4**) were reduced by using Pd/C and hydrazine hydrate and new amine compounds (**5, 6** and **8**) were obtained. The structures of new double-armed crown ether compounds (**2–4**), their metal complexes (**1a–4a, 1b–4b, 2c–4c**) and amine compounds (**5**, **6** and **8**) were elucidated by FTIR, HRMS, ^{1}H–NMR, ^{13}C–NMR spectroscopic methods. The thermal behaviors of these nitro group containing ligands (**1–4**) were compared with the resulting silver complexes (**1c–4c**) and amine compounds (**5**, **6** and **8**). All synthesized compounds were examined for antibacterial activity against pathogenic strains *Listeria monocytogenes*, *Salmonella typhi H*, *Bacillus cereus*, *Staphylococcus aureus*, *Staphylococcus epidermidis*, *Micrococcus luteus*, *Escherichia coli*, *Klebsiella pneumonia*, *Proteus vulgaris*, *Serratia marcescens*, *Shigella dysenteria* and antifungal activity against *Candida albicans*.

Graphical abstract

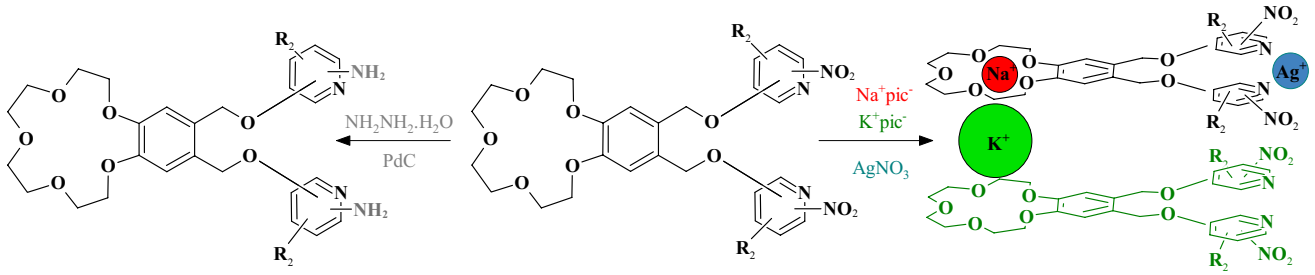

Keywords Crown ethers · Pyridine compounds · Alkali metal complexes · Transition metal complexes · Antimicrobial activity · Thermal analysis

✉ Serhat Koçoğlu
serhatkocoglu@baskent.edu.tr

[1] Food Processing Department, Kahramankazan Vocational School, Başkent University, 06980 Ankara, Turkey

[2] Department of Chemistry, Faculty of Science, Ankara University, 06100 Ankara, Turkey

[3] Department of Field Crops, Faculty of Agriculture, Kırşehir Ahi Evran University, 40100 Kırşehir, Turkey

Introduction

Crown ether compounds have been extensively studied with different ring sizes, heteroatoms, and side groups since Pedersen's discovery in 1967, and they have been used as cation-binding subunits in a variety of applications [1–4]. There are

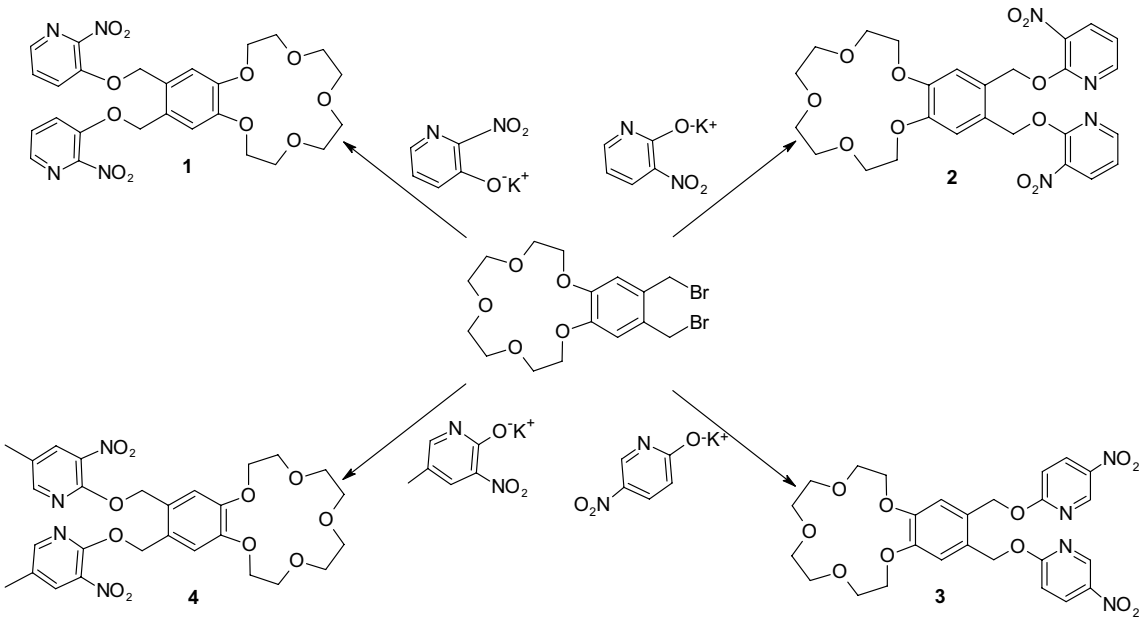

Scheme 1 Structures of new nitropyridine substituted double-armed benzo 15-crown-5 compounds (**1–4**)

many studies showing that many organic molecules containing crown ether units have very high selectivities towards metal ions [5–7]. Crown ether compounds provide the potential for biological activity, as crown ether ligands or Na^+ or K^+ complexes that can interact with Na^+ and K^+ ions can alter the intracellular Na^+/K^+ balance, depending on the ring sizes [8, 9]. In addition, transition metal complexes (such as Ag^+) obtainable if the binding side groups are heterocyclic compounds may also exhibit significant biological activity [10–12].

The 2-pyridyloxy (OPy) group as a directing group is widely used in transition-metal-catalyzed activation and transformation of C–H bonds of aromatic systems [8–11, 13–16].

It is quite common to examine the thermal properties of compounds containing nitro groups [17, 18]. It is possible to observe a noticeable change in the thermal properties of the compounds in which the nitro group containing structures are substituted, the amine compounds obtained by reducing the nitro groups of these compounds, and also the complexes of these compounds with transition metals [19, 20].

In this work we present, the synthesis of nitropyridine-substituted double armed benzo-15-crown-5 ligands (**1–4**) (Scheme 1). These compounds (**1–4**) have two coordinative binding centre (in crown ether cavity and the pyridine unit). Sodium or potassium metal cation was coordinated in crown ether cavity and silver(I) cation was coordinated pyridine unit (Scheme 2). All alkali and transition metal complexes were characterised (**1a–4a, 1b–4b, 1c–4c**) spectroscopic techniques. New amine compounds (**5, 6** and **8**) were obtained from reduced nitro substituded ligands (**1, 2** and **4**) by using Pd/C and hydrazine hydrate. The antimicrobial behaviors of the ligands (**1–8**) and complexes (**1a–4a, 1b–4b, 1c–4c**) were investigated for antibacterial activity against pathogenic strains. In addition, the thermal behaviors of the nitro groups of the synthesized ligands (**1–4**) were compared with the obtained silver complexes (**1c–4c**) and amine compounds (**5, 6** and **8**).

Materials and methods

Physical measurements

All solvents and reagents commercially purchased from Sigma-Aldrich Chemical Company were used without pretreatment unless otherwise stated. Sodium and potassium picrate salts were prepared according to the literature method [21]. Compounds **1a**–**1c** and **5** [22], tetraethylene glycol dichloride [23] benzo-15-crown-5 [1] and 4′,5′-bis(bromomethyl)benzo-15-crown-5 [24] were prepared in accordance with the literature. Melting points were determined with a Electrothermal IA9100 melting point apparatus. ^{1}H– and ^{13}C–NMR spectra were recorded on a Varian Mercury 400 MHz FT-NMR spectrometer (internal standard: $SiMe_4$). The IR spectra were recorded using Shimadzu Infinity FTIR spectrometer with ATR attachment. HRMS spectra were performed on a Agilent Technologies 6224 TOF LC/MS spectrometer. Thermogravimetric measurements were made with Shimadzu

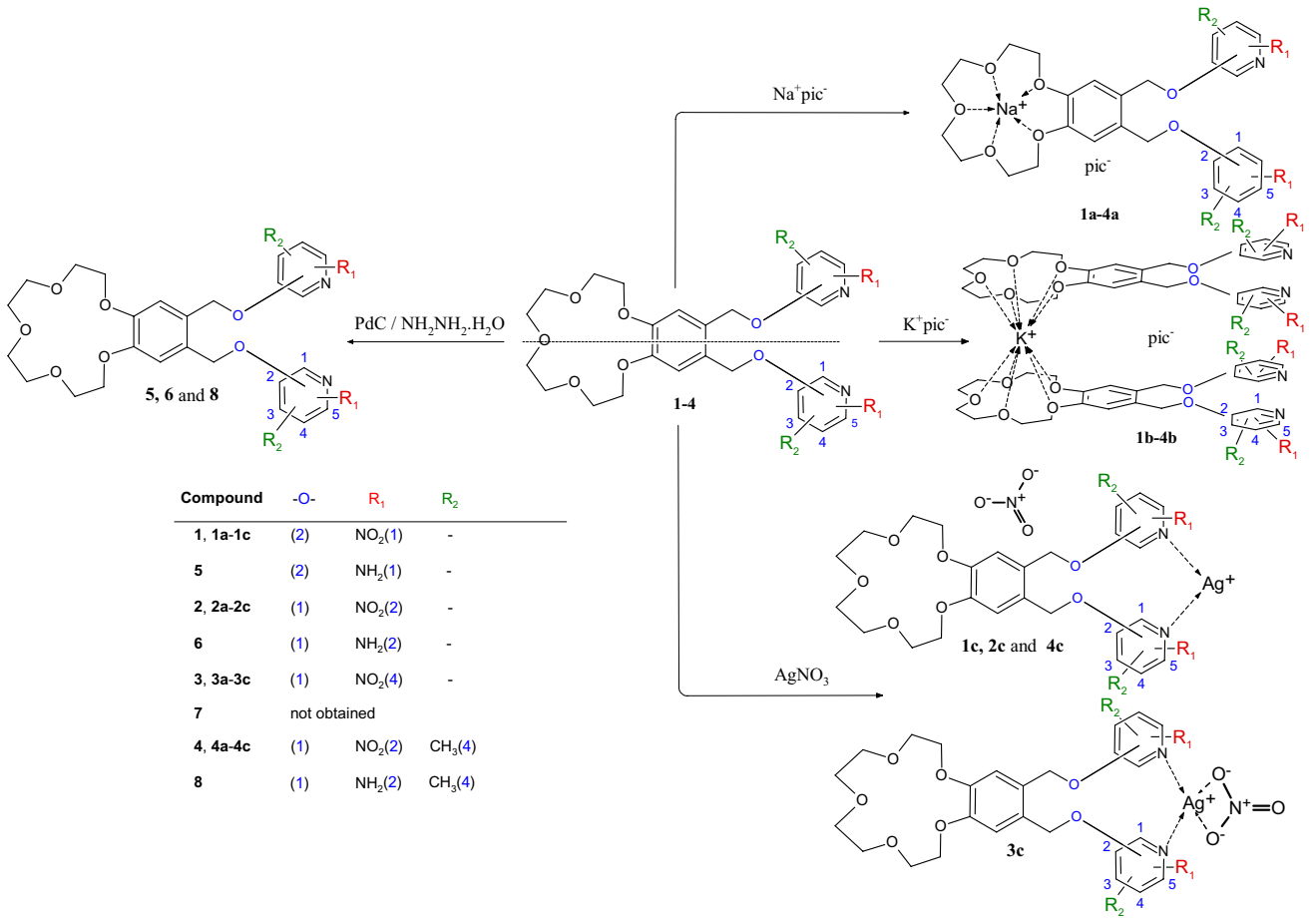

Compound	-O-	R_1	R_2
1, **1a-1c**	(2)	NO_2(1)	-
5	(2)	NH_2(1)	-
2, **2a-2c**	(1)	NO_2(2)	-
6	(1)	NH_2(2)	-
3, **3a-3c**	(1)	NO_2(4)	-
7	not obtained		
4, **4a-4c**	(1)	NO_2(2)	CH_3(4)
8	(1)	NH_2(2)	CH_3(4)

Scheme 2 Structures of new Na^+ (**1a**-**4a**), K^+ (**1b**-**4b**) and $Ag.^+$ (**1c**-**4c**) complexes and amine compunds (**5**, **6**, **8**)

DTG-60 using a platinum pan (heating: 10 °C/min; N_2 atmosphere).

Test microorganisms

The pathogenic (disease agent) bacterial cultures; *Listeria monocytogenes* 4b ATCC19115, *Salmonella typhi H* NCTC901.8394, *Bacillus cereus* RSKK863, *Staphylococcus aureus* ATCC25923, *Staphylococcus epidermidis* ATCC12228, *Micrococcus luteus* ATCC9341, *Escherichia coli* ATCC1280, *Klebsiella pneumonia* ATCC 27,853*, Proteus vulgaris* RSKK 96,026, *Serratia marcescens* sp.*, Shigella dysenteria* type 2 NCTC2966 and a yeast culture were used *Candida albicans* Y-1200-NIH.

Detection of antimicrobial activity

The synthesized compounds were screened for their antimicrobial activity by the well-diffusion method against six Gram-negative bacteria (*S. typhi*, *E.coli*, *K. pneumonia*, *P. vulgaris*, *S. marcescens* sp., *S. dysenteria*), five Gram-positive bacteria (*L. monocytogenes*, *B. cereus*, *S. aureus*, *S. epidermis*, *M. luteus*) and one yeast (*C. albicans*). The compounds were kept dry at room temperature and dissolved (10^3 µM) in DMSO. DMSO was used as solvent for compounds and also for control. DMSO was found to have not antimicrobial activity against any of the microorganisms. 1% (v/v) of the 24 h broth cultures (pathogenic bacteria and yeast) containing 10^6 CFU/mL were placed in sterile plate. Mueller–Hinton Agar (MHA) (15 mL) cooled to 45 °C was poured into plate and released to solidify. Then, the 6 mm diameter wells were carefully drilled with a sterile cork drill and the synthesized compounds were placed and incubated for 24 h at 37 °C on the incubator [25, 26]. Upon completion of the incubation period, the average value obtained for the two wells were used to calculate the zone of growth inhibition of each pathogenic bacteria and yeast (to compare the degree of inhibition, bacteria and yeast were tested for resistance to 4 standard antibiotics (Kanamycin-30 µg: K30; Sulphamethoxazol-25 µg: SXT25; Ampicillin-10 µg: AMP10; Amoxycillin-30 µg: AMC30)and one anticandidal (Nystatin-100 µg: NYS100) [27, 28].

Synthesis of ligand (1–4)

KOH (0.11 g, 2.0 mmol) was dissolved in ethanol (50 mL). The nitropyridine derivatives (3-hydroxy-2-nitropyridine; 2-hydroxy-3-nitropyridine; 2-hydroxy-5-nitropyridine; 2-hydroxy-5-methyl-3-nitropyridine) (2.0 mmol) in DMF was added slowly. After the reaction mixture was refluxed for 2 h, 4′,5′-bisbis(bromomethyl)benzo-15-crown-5 (0.45 g, 1.0 mmol) in DMF (20 mL) was added slowly to the mixture and the resulting solution was stirred over night at room temperature. Then, the oily compound (**1**) was extracted from the solution dicholoromethane:water (1:1) and was recrystallized from *n*-hexane [22]. For compounds **2** and **3** the solution turned clear after water was added, and then the solution extracted with chloroform several times. The chloroform extract was dried over $MgSO_4$ and filtered. The filtered solution was evaporated and the remaining precipitate (yellow for compound **2**, white for compound **3**) crystallized with acetonitrile. For compound **4** yellow residue was observed with the addition of water. After that, the resulting yellow solid was filtered and crystallized with acetonitrile. **1**: mp = 201 °C (Yield: 72%) [22]; **2**: mp = 157 °C (Yield: 64%); **3**: mp = 271 °C (Yield: 61%); **4**: mp = 139 °C (Yield: 78%).

Synthesis of sodium complexes (1a-4a)

Sodium picrate (25.1 mg, 0.1 mmol) was added to the corresponding ligand (**1–4**) (0.1 mmol) dissolved in acetone (10 mL) and and refluxed for 2 h. The resulting complex was filtered and recrystallized from EtOH. **1a:** mp = 161 °C (Yield: 58%) [22]; **2a**: mp = 246 °C (Yield: 59%); **3a**: mp = 229 °C (Yield: 54%); **4a**: mp = 293 °C (Yield: 62%).

Synthesis of potassium complexes (1b-4b)

Potassium picrate (13.4 mg, 0.05 mmol) was added to the corresponding ligand (**1–4**) (0.1 mmol) dissolved in acetone (10 mL) and refluxed for 2 h. The resulting complex was filtered and recrystallized from EtOH. **1b:** mp = 175 °C (Yield: 64%) [22]**; 2b:** mp = 227 °C (Yield: 62%); **3b:** mp = 242 °C (Yield: 59); **4b:** mp = 264 °C (Yield: 72%).

Synthesis of Ag(I) complexes (1c-4c)

$AgNO_3$ (170 mg, 1.00 mmol) was added to the corresponding ligand (**1–4**) (1.00 mmol) dissolved in EtOH (10 mL) and stirred overnight at room temperature (~25 °C). Diethyl ether was added to the solution and stirring was continued for about 1 more hour. The resulting complex was filtered and recrystallized from CH_2Cl_2. **1c**: mp = 197 °C (Yield: 63%) [22]; **2c:** mp = 140 °C (Yield: 54%); **3c**: mp = 195 °C (Yield: 51%); **4c:** mp = 181 °C (Yield: 58%).

Reduction of nitro groups to amines (5, 6 and 8)

The corresponding crown ether (**1, 2** and **4**) (1.00 mmol) was dissolved in EtOH (5 mL). Then Pd–C (m/m %10) was added and hydrazine hydrate was dropped slowly and than the solution was refluxed around 4 h. The crude compound was filtered and recrystallized from ethanol. **5**: mp = 161 °C (Yield: 56%); **6**: mp = 94 °C (Yield 46%); **8**: mp = 89 °C (Yield: 49%).

Results and discussion

Synthesis and structural characterisations

This study consisted of three different reaction steps. Firstly, crown ether ligands **1** [22] and **2–4** were obtained from the reaction of the starting compound 4′,5′bis-(bromomethyl)-benzo-15-crown-5 with hydroxypyridine derivatives in DMF with KOH (Scheme 1).

Then, complexes (**1a–4a, 1b–4b, 1c–4c**) of **1** [22] and new compounds (**2–4**) with alkali (Na^+ and K^+) and transition (Ag^+) metal complexes were obtained (Scheme 2). Reactions were carried out in ethanol by using sodium picrate for sodium complexes (**1a–4a**) and potassium picrate for potassium complexes (**1b–4b**). It was observed that the solubility of the synthesized complexes (**2a–4a**, **2b–4b, 2c–4c**) was quite low compared to the solubility of the ligands. Sodium and potassium give an inclusion complex with the crown ether part, while the transition metal is complexed with the side arms of the ligand (Scheme 2). The radius of the Na^+ ion conforms to the 15 crown-5 cavity, and thus forms 1:1 metal:ligand complexes, while the K^+ ion's radius is usually larger than the 15 crown-5 cavity, thus forming 1:2 metal:ligand sandwich-type complexes [29, 30]. Ag^+ complexes (**1c–4c**) were synthesized with $AgNO_3$ in ethanol. In complexes **1c** [22], **2c** and **4c**, silver(I) ion was surrounded by two nitrogen atoms of the ligand and form a bi-coordinated structure, while in complex **3c**, surrounded by two nitrogen atoms of the ligand and nitrate anion, it form a four-coordinated structure. HRMS and NMR spectral data confirm the proposed structures.

In the final reaction step in this study, new amine compounds (**5**, **6** and **8**) were obtained from reduced nitro substituted ligands (**1**, **2** and **4**) by using Pd/C and hydrazine hydrate. The compound that was intended to be obtained by reduction of compound **3**, symbolized by number **7**, could not be obtained.

Mass spectra

The HRMS spectral data of the ligands (**1–6** and **8**) and complexes (**1a–4a, 1b–4b, 1c–4c**) were detected. The mass spectral data (measured and calculated molecular ion peaks and error ratios) of the compounds are given in Table 1.

The molecular ion peak $[M+Na]^+$ at m/z 595.16668, 595.16609 and 623.19841 supports the proposed structure of the **2–4**, respectively (Fig. S1). In the mass spectra of all ligands (**1–4**), it was observed that sodium ion was attached to the structure. It is quite common in HRMS spectra to see molecular ion peaks where sodium ion participates in the structure [13, 14, 22, 31, 32].

Mass spectra of the Na^+ and K^+ complexes (**1a–4a, 1b–4b**) showed that the sodium metal binds to the ligand structure in such a way as to form a 1:1 (metal:ligand) "filling complex" and potassium metal forming a 1:2 (metal:ligand) "sandwich complex" (Fig. S2).

Mass spectra have provided very useful evidence for elucidating the structures of Ag(I) complexes (**1c–4c**). The molecular ion peak of the complexes supports the proposed structure. M and M + 2 isotope peaks (51.84% ^{107}Ag, 48.16% ^{109}Ag) from the Ag(I) atom were recorded in the spectra. In Ag(I) isotope peak patterns, the ratio of peaks is 1:1 as expected.. In the mass spectra show that the M and M + 2 peaks at m/z 679.07780 and 681.07887 (for compound **1c**) [22], 679.07788 and 681.07774 (for compound **2c**), 707.11305 and 709.11343 (for compound **4c**) (Fig. S3). These spectra suggested that the Ag(I) complex formed two-coordinated structure with the ligand (Scheme 2). In the mass spectrum of compound **3c**, the M and M + 2 peaks were detected at m/z 764.05742 and 766.05812 correspond to the ligand plus sodium and nitrate ($[M+Na+NO_3]^+$). The observation of the molecular ion peak including the nitrate anion, showed that the Ag(I) complex formed was four coordinated (Scheme 2). In addition, in the spectrum of compound **3c**, as in the spectrum of ligands (**2–4**), sodium ion is also seen in the structure.

Molecular ion peaks ($[M+Na]^+$) were observed at m/z 535.21488, 535.21482 and 5633.24613 in the mass spectra of compounds **5**, **6** and **8** obtained by reduction of compounds **1**, **2** and **4**. This proved that reduction had taken place and new amine compounds (**5**, **6** and **8**) were formed.

FTIR spectra

IR data for ligands (**1–6** and **8**) and complexes (**1a–4a, 1b–4b** and **1c–4c**) are summarized in Table 2. The most characteristic peaks of crown ether are aromatic and aliphatic ν(COC) vibrations, and these peaks were observed in compounds **1–6** and **8** at 1300–1209 and 1146–1049 cm^{-1}.

Table 1 Mass spectral data (in CH_3CN)

Compound	Molecular ion	Mass (measured)	Mass (calculated)	(ppm)
1	$[M+Na]^+$	595.16423	595.16529	1.78
2	$[M+Na]^+$	595.16668	595.16529	−2.34
3	$[M+Na]^+$	595.16609	595.16529	−1.34
4	$[M+Na]^+$	623.19841	623.19659	−2.92
1a	$[M]^+$	595.16325	595.16529	3.43
2a	$[M]^+$	595.16285	595.16529	4.10
3a	$[M]^+$	595.16369	595.16529	2.69
4a	$[M]^+$	623.19492	623.19659	2.68
1b	$[M]^+$	1183.30812	1183.31474	5.59
2b	$[M]^+$	1183.30901	1183.31474	4.84
3b	$[M]^+$	1183.30883	1183.31474	4.99
4b	$[M]^+$	1239.37245	1239.37734	3.95
1c	$[M]^+$	679.07780	679.08062	4.15
	$[M+2]^+$	681.07887	681.08027	2.06
2c	$[M]^+$	679.07788	679.08062	4.03
	$[M+2]^+$	681.07774	681.08027	3.71
3c	$[M+Na+NO_3]^+$	764.05742	764.05822	1.05
	$[M+2+Na+NO_3]^+$	766.05812	766.05787	−0.33
4c	$[M]^+$	707.11305	707.11192	−1.60
	$[M+2]^+$	709.11343	709.11157	−2.62
5	$[M+Na]^+$	535.21488	535.21691	3.79
6	$[M+Na]^+$	535.21482	535.21691	3.91
8	$[M+Na]^+$	563.24613	563.24821	3.69

Table 2 Selected IR bands of compounds (ν cm^{-1})

Comp	ν(C=C)	$\nu(NO_2)$	$\nu(C{=}N)_{pyr}$	$\nu(C{-}O{-}C)_{ar}$	$\nu(C{-}H)_{al}$	$\nu(C{-}O{-}C)_{al}$	Pic.
1	1562;1452(m)	1526;1367(s)	1599(m)	1265;1227(s)	2934;2864(w)	1117;1053(s)	
2	1599;1452(m)	1518;1348(s)	1668(s)	1252;1209(s)	2870(w)	1132;1090(s)	
3	1614;1491(m)	1524;1321(s)	1672(s)	1267;1244(s)	2949;2864(w)	1121;1082(s)	
4	1607;1450(m)	1518;1344(s)	1672(s)	1269;1229(s)	2920;2866(w)	1101;1049(s)	
1a	1601;1460(m)	1524;1333(s)	1639(s)	1271;1213(s)	2924;2878(w)	1116;1103(s)	1639(s)
2a	1601;1470(m)	1522;1348(s)	1676(s)	1254;1223(s)	2916;2878(w)	1113;1072(s)	1630(s)
3a	1612;1491(m)	1522;1321(s)	1670(s)	1267;1244(s)	2949;2866(w)	1121;1080(s)	1636(m)
4a	1609;1464(s)	1518;1352(s)	1681(s)	1298;1256(s)	2932;2878(w)	1120;1105(s)	1633(s)
1b	1601;1460(s)	1524;1364(s)	1641(s)	1272;1216(s)	2916;2880(w)	1117;1072(s)	1641(s)
2b	1593;1470(s)	1518;1348(s)	1672(s)	1287;1254(s)	2937;2874(w)	1115;1072(s)	1638(s)
3b	1614;1491(m)	1522;1321(s)	1670(s)	1267;1244(s)	2949;2867(w)	1120;1082(s)	1614(s)
4b	1607;1464(s)	1518;1352(s)	1682(s)	1298;1258(s)	2930;2872(w)	1121;1072(s)	1636(s)
1c	1562;1462(m)	1530;1350(s)	1599(m)	1273;1238(s)	2934;2872(w)	1146;1105(s)	
2c	1599;1462(m)	1518;1348(s)	1668(s)	1248;1209(s)	2874(w)	1132;1090(s)	
3c	1560;1445(s)	1523;1346(s)	1672(s)	1269;1244(s)	2949;2864(w)	1121;1082(s)	
4c	1603;1296(s)	1528;1296(s)	1672(s)	1296;1225(s)	2870(w)	1123;1096(s)	
5	1562;1462(s)	–	1629(s)	1273;1238(s)	2934;2872(w)	1146;1105(s)	
6	1582;1450(s)	–	1641(s)	1267;1221(m)	2920;2864(w)	1125;1061(s)	
8	1582;1447(s)	–	1653(m)	1300;1265(s)	2920;2886(w)	1126;1111(s)	

w weak, *m* medium, *s* strong, $\nu(NH_2)$ ***5*** 3318 cm^{-1}, **6** 3327 cm^{-1}, **8** 3336 cm^{-1}

Other characteristic $\upsilon_{(C-H)}$, $\upsilon_{(C=C)}$ and $\upsilon_{(C=N)}$ peaks were recorded in the expected regions (Table 2). While the NO_2 vibration peaks in nitro-substituted compounds (**1–4**) were observed as a sharp peak in 1526; 1367 (for compound **1**) [22] 1518; 1348 (for compound **2**), 1524; 1321 (for compound **3**) and 1518; 1344 (for compound **4**), these peaks disappeared in amine-reduced compounds (**5, 6** and **8**). In the IR spectra of the amine compounds (**5, 6** and **8**), the characteristic internal $\nu(NH_2)$ absorption bands were observed at 3318, 3327 and 3336 cm^{-1} (N–H stretching), respectively.

It was observed that the IR spectra of alkali metal complexes (**1a–4a** and **1b–4b**) and the IR spectra of free ligands (**1–4**) were similar to each other. The presence of picrate is indicated by the characteristic very strong bands at 1639, 1630, 1636, 1633 and 1641, 1638, 1614, 1636 cm^{-1} for compounds (**1a–4a** and **1b–4b**), respectively.

The IR spectra of Ag(I) complexes (**1c–4c**) were compared with ligands spectra to identify possible changes that might have occurred with the complexation. However, it was observed that the IR spectra of Ag(I) complexes (**1c–4c**) were not very different from the ligand spectra. Only in the spectrum of **3c**, a broad peak intensity was observed in the range of 1346–1244 cm^{-1} due to the coordination of the nitrate anion to the structure.

^{1}H- and ^{13}C-NMR spectra

Synthesized ligands (**1–6** and **8**) and complexes (**1a–4a**, **1b–4b** and **1c–4c**) ^{1}H–NMR spectral data are summarized in Tables 3, 4, 5. All molecules are symmetrical, so in Tables 3 and 4 the number of proton peaks was evaluated by considering half the molecule. In compounds **1–6** and **8**, characteristic peaks belonging to the 15-crown-5 group ($-OCH_2-CH_2O-$) (H10–H13) were observed as multiple peaks in betwen of $\delta = 3.57–4.91$ ppm (Figs. S4–S10). The other most characteristic peak, aliphatic $-CH_2-$ protons (H6), were recorded as a singlet peak in each compound (**1–6** and **8**). The $-CH_3$ proton (H14) peaks for compounds **4** and **8** were observed as a singlet peak at $\delta = 2.16$ and 1.92 ppm, respectively. The peaks of aromatic protons (H2–H5) of all compounds (**1–6** and **8**) were observed in the expected regions and as expected peak multiplicities (Table 3). Aromatic H8 proton was observed as a singlet in all compounds (**1–6** and **8**). When amine compounds (**5**, **6** and **8**) and nitro compounds (**1**, **2** and **4**) were compared, it was determined that all aromatic proton peaks shifted to higher field as expected. In addition, the peaks of NH_2 protons in compounds **5**, **6** and **8** were detected at $\delta = 4.65$, 4.21 and 4.18 ppm, respectively.

The ^{1}H–NMR spectra of the alkali metal (Na^+ and K^+) complexes (**1a–4a** and **1b–4b**) showed similar spectra to the ligands (**1–4**), which are the starting compounds

Table 3 ^{1}H-NMR spectral data of the compounds (1–6 and 8) (δ, ppm)

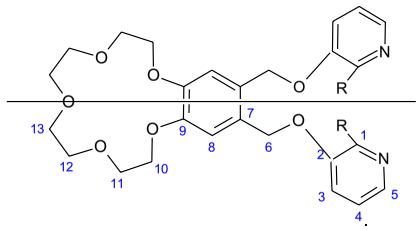

Compound	R
(1)	NO_2
(5)	NH_2

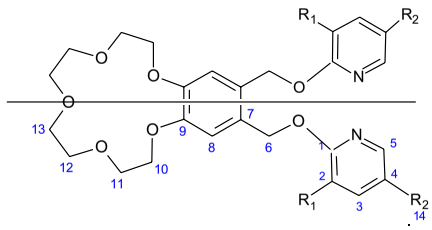

Compound	R_1	R_2
(2)	NO_2	H
(3)	H	NO_2
(4)	NO_2	CH_3
(6)	NH_2	H
(8)	NH_2	CH_3

Compound	H2	H3	H4	H5	H6	H8	H10	H11	H12	H13	H14	NH_2
1[a]	–	7.66 (d; 2H) $^{2}J_{4\text{-}3}$: 8.20 Hz	7.55 (dd; 2H) $^{2}J_{5\text{-}4}$: 4.69 Hz $^{2}J_{3\text{-}4}$: 8.21 Hz	8.10 (dd; 2H) $^{2}J_{4\text{-}5}$: 4.69 Hz $^{3}J_{3\text{-}5}$: 1.17 Hz	5.29 (s; 4H)	7.04 (s; 2H)	4.18 (t; 4H)	3.91 (t; 4H)	3.74 (t; 8H)		–	–
2[b]	–	8.15 (dd; 2H) $^{2}J_{4\text{-}3}$: 7.82 Hz $^{3}J_{5\text{-}3}$: 1.95 Hz	6.41 (t; 2H) $^{2}J_{5\text{-}4}$: 7.05 Hz $^{2}J_{3\text{-}4}$: 7.05 Hz	8.39 (dd; 2H) $^{2}J_{4\text{-}5}$: 6.85 Hz $^{3}J_{3\text{-}5}$: 1.76 Hz	5.29 (s; 4H)	6.87 (s; 2H)	3.99 (t, 4H)	3.72 (t; 4H)	3.57 (t; 8H)		–	–
3[b]	6.46 (d; 2H) $^{2}J_{3\text{-}2}$: 9.77 Hz	8.09 (dd; 2H) $^{2}J_{2\text{-}3}$: 10.16 Hz $^{3}J_{5\text{-}3}$: 3.13 Hz	–	8.94 (d; 2H) $^{3}J_{3\text{-}5}$: 3.13 Hz	5.24 (s; 4H)	6.92 (s; 2H)	4.00 (t, 4H)	3.72 (t; 4H)	3.57 (t; 8H)		–	–
4[b]	–	7.92 (d; 2H) $^{3}J_{5\text{-}3}$: 2.00 Hz	–	8.28 (d; 2H) $^{3}J_{3\text{-}5}$: 2.34 Hz	5.23 (s; 4H)	6.89 (s; 2H)	4.00 (t, 4H)	3.73 (t; 4H)	3.57 (t; 8H)		2.05 (s; 6H)	–
5[a]	–	6.95 (dd; 2H) $^{2}J_{4\text{-}3}$: 7.82 Hz $^{3}J_{5\text{-}3}$: 1.17 Hz	6.57 (dd; 2H) $^{2}J_{5\text{-}4}$: 5.08 Hz $^{2}J_{3\text{-}4}$: 7.82 Hz	7.66 (dd; 2H) $^{2}J_{4\text{-}5}$: 5.08 Hz $^{3}J_{3\text{-}5}$: 1.17 Hz	5.04 (s; 4H)	6.96 (s; 2H)	4.16 (t; 4H)	3.91 (t; 4H)	3.75 (t; 8H)		–	4.65 (s; 4H)
6[a]	–	6.50 (dd; 2H) $^{2}J_{4\text{-}3}$: 7.04 Hz $^{3}J_{5\text{-}3}$: 1.57 Hz	6.03 (t; 2H) $^{2}J_{5\text{-}4}$: $^{2}J_{5\text{-}4}$: 7.04 Hz $^{2}J_{3\text{-}4}$: 7.04 Hz	6.61 (dd; 2H) $^{2}J_{4\text{-}5}$: 7.23 Hz $^{3}J_{3\text{-}5}$: 1.76 Hz	5.17 (s; 4H)	6.68 (s; 2H)	4.04 (t; 4H)	3.85 (t; 4H)	3.71 (t; 8H)		–	4.21 (s; 4H)
8[a]	–	6.28 (d; 2H) $^{3}J_{5\text{-}3}$: 1.17 Hz	–	6.37 (d; 2H) $^{3}J_{3\text{-}5}$: 1.95 Hz	5.12 (s; 4H)	6.71 (s; 2H)	4.06 (t, 4H)	3.86 (t; 4H)	3.72 (t; 8H)		1.92 (s; 6H)	4.18 (s; 4H)

s: singlet, *d:* doublet, *t:* triplet, *dd:* doublet of doublets, *m:* multiplet; *a:* $CDCl_3$, *b:* DMSO-d_6

Table 4 ^{1}H-NMR spectral data of the alkali metal complexes (**1a–4a**, **1b–4b**) (δ, ppm)

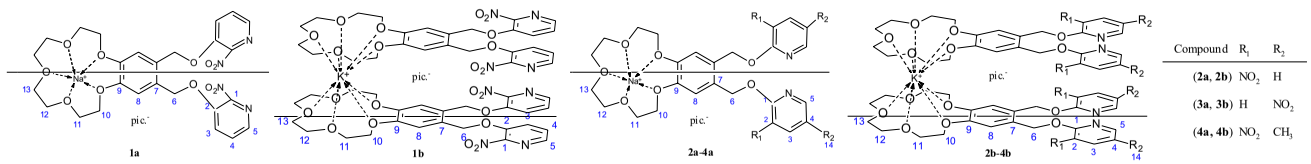

Compound	H2	H3	H4	H5	H6	H8	H10	H11	H12	H13	H14	Picrate
1a[a]	–	7.70 (d; 2H) $^{2}J_{4\text{-}3}$: 8.47 Hz	7.59 (dd; 2H) $^{2}J_{5\text{-}4}$: 4.40 Hz $^{2}J_{3\text{-}4}$: 8.47 Hz	8.13 (dd; 2H) $^{2}J_{4\text{-}5}$: 4.40 Hz $^{3}J_{3\text{-}5}$: 1.17 Hz	5.30 (s; 4H)	7.12 (s; 2H)	4.27 (t; 4H)	4.04 (t; 4H)	3.82 (m; 4H)	3.80 (m; 4H)	–	8.82
2a[b]	–	8.15 (dd; 2H) $^{2}J_{4\text{-}3}$: 6.65 Hz $^{3}J_{5\text{-}3}$: 1.96 Hz	6.42 (dd; 2H) $^{2}J_{3\text{-}4}$: 7.04 Hz $^{2}J_{5\text{-}4}$: 7.62 Hz	8.40 (dd; 2H) $^{2}J_{4\text{-}5}$: 7.62 Hz $^{3}J_{3\text{-}5}$: 2.15 Hz	5.29 (s; 4H)	6.88 (s; 2H)	4.00 (t, 4H)	3.73 (t; 4H)	3.58 (t; 8H)		–	8.59
3a[b]	6.47 (d; 2H) $^{2}J_{3\text{-}2}$: 9.77 Hz	8.09 (dd; 2H) $^{2}J_{2\text{-}3}$: 9.77 Hz $^{3}J_{5\text{-}3}$: 3.12 Hz	–	8.95 (d; 2H) $^{3}J_{3\text{-}5}$: 3.12 Hz	5.25 (s; 4H)	6.93 (s; 2H)	4.01 (t, 4H)	3.73 (t; 4H)	3.57 (t; 8H)		–	8.58
4a[b]	–	7.67 (d; 2H) $^{3}J_{5\text{-}3}$: 2.35 Hz	–	8.29 (d; 2H) $^{3}J_{3\text{-}5}$: 2.34 Hz	5.23 (s; 4H)	6.89 (s; 2H)	4.00 (t, 4H)	3.73 (t; 4H)	3.58 (t; 8H)		2.05 (s; 6H)	8.58
1b[a]	–	7.82 (m; 4H)	7.58 (dd; 4H) $^{2}J_{5\text{-}4}$: 4.25 Hz $^{2}J_{3\text{-}4}$: 8.41 Hz	8.10 (d; 4H) $^{2}J_{4\text{-}5}$: 4.25 Hz	5.35 (s; 8H)	7.02 (s; 4H)	3,80 (m; 8H)	3.73 (m; 24H)			–	8.78
2b[b]	–	8.15 (dd; 4H) $^{2}J_{4\text{-}3}$: 6.64 Hz $^{3}J_{5\text{-}3}$: 2.35 Hz	6.43 (t; 4H) $^{2}J_{3\text{-}4}$: 6.64 Hz $^{2}J_{5\text{-}4}$: 7.23 Hz	8.39 (dd; 4H) $^{2}J_{4\text{-}5}$:7.81 Hz $^{3}J_{3\text{-}5}$: 1.95 Hz	5.29 (s; 8H)	6.74 (s; 4H)	4.00 (t, 8H)	3.73 (t; 8H)	3.58 (t; 16H)		–	8.59
3b[b]	6.47 (d; 2H) $^{2}J_{3\text{-}2}$: 10.16 Hz	8.11 (dd; 4H) $^{2}J_{2\text{-}3}$: 9.77 Hz $^{3}J_{5\text{-}3}$: 2.16 Hz	–	8.95 (m; 4H)	5.26 (s; 8H)	6.94 (s; 4H)	4.02 (m, 8H)	3.73 (m; 8H)	3.58 (mt; 16H)		–	8.58
4b[b]	–	7.92 (d; 4H) $^{3}J_{5\text{-}3}$: 2.35 Hz	–	8.29 (d; 4H) $^{3}J_{3\text{-}5}$: 1.96 Hz	5.23 (s; 8H)	6.89 (s; 4H)	4.01 (t, 8H)	3.73 (t; 8H)	3.32 (t; 16H)		2.05 (s; 12H)	8.58

s: singlet, *d:* doublet, *t:* triplet, *dd:* doublet of doublets, *m:* multiplet; *a:* $CDCl_3$, *b:* DMSO-d_6

Table 5 ^{1}H-NMR spectral data of the ligand (**1c–4c**) (δ, ppm)

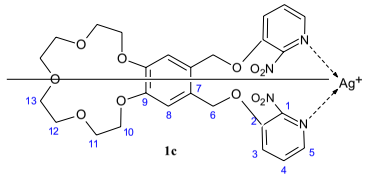

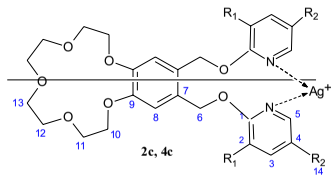

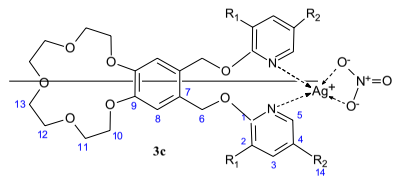

Compound	R_1	R_2
(2c)	NO_2	H
(3c)	H	NO_2
(4c)	NO_2	CH_3

Compound	H2	H3	H4	H5	H6	H8	H10	H11	H12	H13	H14
1c[a]		7.66 (d; 2H) $^{2}J_{4\text{-}3}$: 7.81 Hz	7.55 (m; 2H)	8.11 (d; 2H) $^{2}J_{4\text{-}5}$: 4.29 Hz	5.31 (s; 4H)	7.05 (s; 2H)	4.19 (t; 4H)	3.93 (t; 4H)	3.76 (m; 8H)		–
2c[b]	–	8.13 (dd; 2H) $^{2}J_{4\text{-}3}$: 6.64 Hz $^{3}J_{5\text{-}3}$: 1.95 Hz	6.41 (t; 2H) $^{2}J_{3\text{-}4}$: 6.84 Hz $^{2}J_{5\text{-}4}$: 7.23 Hz	8.37 (dd; 2H) $^{2}J_{4\text{-}5}$:7.62 Hz $^{3}J_{5\text{-}5}$: 2.15 Hz	5.27 (s; 4H)	6.86 (s; 2H)	3.98 (t; 4H)	3.71 (t; 4H)	3.56 (m; 8H)		–
3c[b]	6.47 (d; 2H) $^{2}J_{3\text{-}2}$: 10.16 Hz	8.10 (dd; 2H) $^{2}J_{2\text{-}3}$: 9.97 Hz $^{3}J_{5\text{-}3}$: 2.93 Hz	–	8.94 (d; 2H) $^{3}J_{3\text{-}5}$: 3.12 Hz	5.25 (s; 4H)	6.93 (s; 2H)	4.01 (t; 4H)	3.73 (t; 4H)	3.57 (t; 8H)		–
4c[b]	–	7,91 (d; 2H) $^{3}J_{5\text{-}3}$: 1.56 Hz $^{3}J_{5\text{-}3}$: 1.56 Hz	–	8.28 (d; 2H) $^{3}J_{3\text{-}5}$: 2.35 Hz $^{3}J_{3\text{-}5}$: 2.35 Hz	5.23 (s; 4H)	6.89 (s; 2H)	4.01 (t; 4H)	3.73 (t; 4H)	3.58 (t; 8H)		2.05 (s; 6H)

s: singlet, *d:* doublet, *t:* triplet, *dd:* doublet of doublets, *m:* multiplet; *a:* $CDCl_3$, *b:* DMSO-d_6

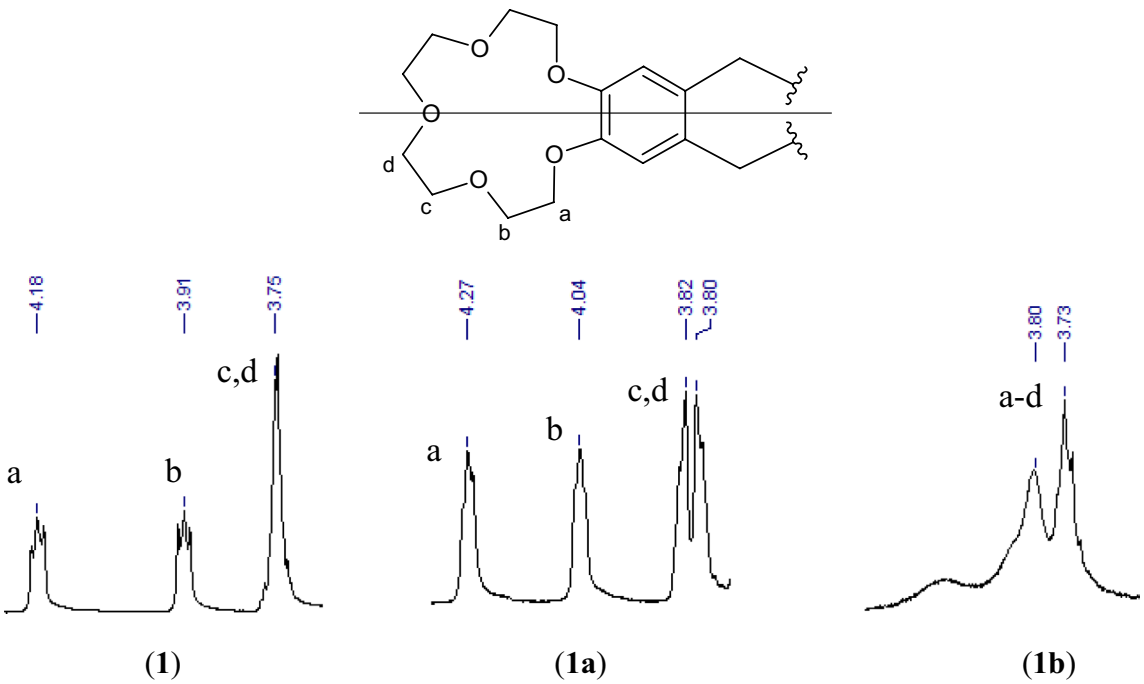

Fig.1 ^{1}H-NMR spectra of crown ether peaks (–OCH_2–CH_2O–) region for ligand (**1**), sodium (**1a**) and potassium complexes (**1b**)

of these complexes (Table 4). Although the synthesized ligands (**2**, **4**) were soluble in $CDCl_3$, ^{1}H–NMR spectra were recorded in DMSO–d_6 because their complexes (**2a**, **2b**, **4a** and **4b**) were not sufficiently soluble in this solvent. In particular, in the spectra recorded in $CDCl_3$, the crown ether proton peaks differently from the free ligand [11, 22, 33–36]. Four equal peak abundances were observed in the synthesized sodium complex (**1a**), while a more mixed peak abundance was observed in the potassium complex (**1b**) (Fig. 1). However, this differentiation observed in the crown ether crest region was not observed in the spectra recorded in DMSO-d_6. The proton peaks of the picrate anion of the Na^+ and K^+ complexes (**1a–4a** and **1b–4b**) were recorded as single peaks at 8.82, 8.59, 8.58, 8.58 and 8.78, 8.59, 8.58, 8.58 ppm, respectively. Integral ratios of picrate protons showed that Na^+ complexes (**1a–4a**) complexed in a ratio of 1:1 (metal:ligand) and K^+ complexes (**1b–4b**) in a ratio of 1:2 (metal:ligand).

The synthesized silver(I) complexes (**1c–4c**) ^{1}H–NMR spectral data are summarized in Table 5. With the complexation, shifts are expected, especially in the aromatic proton peak region. However, it was observed that the spectra of the complexes (**1c–4c**) did not have much shifts and were almost similar to the spectra of the ligands (**1–4**) (Figs. S11–S14). This showed that the silver atom attached to the pyridine nitrogen did not affect the electron density of the aromatic ring protons.

The ^{13}C–NMR spectral data for compounds (**1–6, 1a–4a, 1b–4b** and **1c–4c**) were given in Table 6. Crown ether carbons (C_{10}–C_{13}) were recorded as four peaks in the range of 68–72 ppm in all compounds. Aliphatic –CH_2 carbons (C6) were detected in crown ether carbon peaks region. The –CH_3 carbon (C14) peak in compounds **4, 4a, 4b** and **4c** were observed at 16.87, 16.59, 16.59 and 16.59 ppm, respectively. In addition, the peaks of all aromatic carbons were determined in the expected regions and numbers. The ^{13}C–NMR spectra of the Na^+, K^+ and Ag(I) complexes (**1a–4a**, **1b–4b** and **1c–4c**) were found to be very similar to the corresponding ligands (**1–4**) spectra (Figs. S15–S18).

Antibacterial activities

The considered compounds showed variable activity (11–30 mm) on the growth of used the pathogenic microorganisms and the activity mainly differed between moderate and high activities. In addition, it was determined that the activities of the synthesized compounds in Gram-negative bacteria were more effective than in Gram-positive bacteria (Figs. 2 and 3). Antimicrobial activity data shown in Table 7 were discussed as follows:

(i) Compounds **2, 4b,** and **4c** showed higher inhibitory activity against *L. monocytogenes* (Fig. 2)
(ii) Compounds **1, 1c, 5, 2, 2c** and **4c** showed high antimicrobial activity in *S. typhi* (Fig. S19). Also **4c**

Table 6 ^{13}C-NMR spectral data of the complexes (**1–6**, **1a–4a**, **1b–4b**, **1c–4c**) (δ, ppm)

Compound	C1	C2	C3	C4	C5	C6	C7	C8	C9	C10–C13	C14	Picrate
(1)	149.34	148.87	125.87	124.04	146.48	69.14	128.87	115.21	139.59	69.38; 69.40; 70.41; 71.02	–	
(2)	154.21	148.97	139.27	104.22	145.97	50.00	127.28	115.52	138.50	69.05; 69.05; 70.09; 70.77	–	
(3)	160.82	118.29	130.17	133.27	148.60	49.46	126.40	115.41	140.60	68.63; 68.71; 69.72; 70.35	–	
(4)	153.46	143.71	113.13	137.83	148.95	50.08	127.30	115.85	140.68	69.05; 69.14 70.14; 70.83	16.59	
(1a)	148.81	147.31	126.74	124.14	146.41	67.64	129.03	113.92	139.80	68.10; 69.00; 69.14; 69.39	–	127.02
(1b)	148.38	148.22	125.44	125.15	145.81	68.36	129.50	114.89	139.41	68.41; 68.54; 69.55; 70.29	–	126.46
(1c)	148.38	148.29	126.44	125.44	145.81	68.41	129.50	114.89	139.40	68.46; 68.64; 69.68; 70.42	–	
(5)	149.17	150.17	117.22	115.55	141.28	67.99	127.72	113.64	139.19	69.12; 69.38; 70.39; 70.98	–	
(2a)	154.21	149.00	139.18	104.19	145.89	49.99	127.31	115.63	138.60	69.09; 70.09; 70.74	–	125.59
(2b)	154.21	149.02	139.18	104.19	145.88	50.00	127.29	115.62	138.61	69.09; 69.11 70.10; 70.76	–	125.58
(2c)	154.20	148.91	139.27	104.24	145.98	50.00	127.33	115.52	138.53	68.99; 69.96; 70.63; 70.69		
(6)	157.41	146.34	124.22	107.11	148.45	48.34	128.84	115.21	138.93	69.18;70.23; 70.77;70.79		
(3a)	161.35	118.83	130.69	133.81	149.09	49.99	126.94	115.93	141.12	69.13; 69.21; 70.20; 70.84		125.54
(3b)	161.35	118.81	130.68	133.83	149.04	50.00	126.92	115.84	141.16	69.09; 69.13; 70.16; 70.81		125.58
(3c)	161.35	118.79	130.64	133.83	149.00	49.98	126.85	115.78	141.14	69.06; 69.09; 70.16; 70.85		
(4a)	153.46	143.68	113.12	137.86	148.93	50.08	127.31	115.86	140.66	69.03; 69.11; 70.10; 70.79	16.59	125.62
(4b)	153.46	143.68	113.11	137.87	148.94	50.08	127.30	115.86	140.66	69.03; 69.10; 70.11; 70.79	16.59	
(4c)	153.46	143.67	113.13	137.89	149.01	50.00	127.30	115.92	140.63	69.12; 69.18; 70.21; 70.88	16.59	125.62

(**8**) The peaks could not be observed very clearly because the solubility was too low

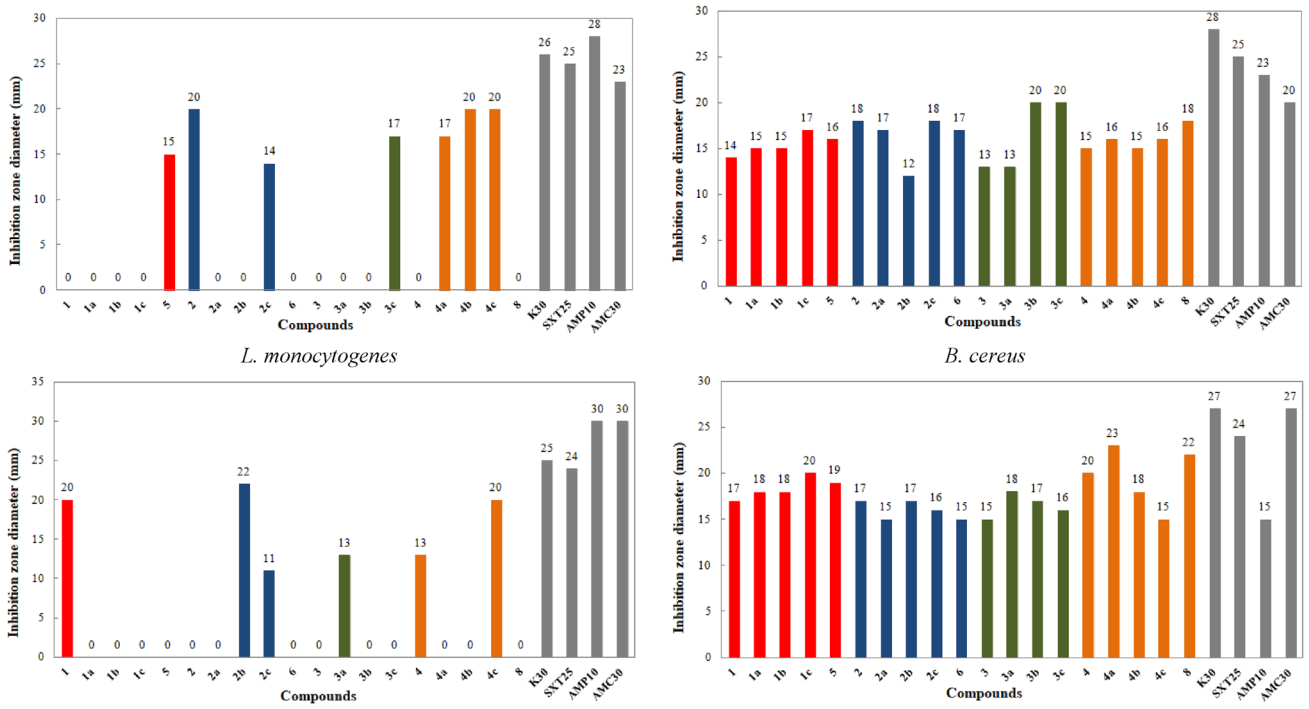

Fig. 2 Antimicrobial activity of synthesized compounds and standard reagents (inhibition zone diameter: mm)

showed a greater inhibitory effect than reference drug K30 (25 mm) and SXT25 (24 mm) in Gram-negative *S. typhi* (Fig. 3). Salmonella serovars cause a wide variety of clinical symptoms in infants, adults and some high-sensitivity animals, from asymptomatic infection to severe typhoid-like syndromes [37, 38]. Compounds **3b** and **3c** showed high inhibitory activity in *B. cereus* (Fig. 2). The bacteria is known as

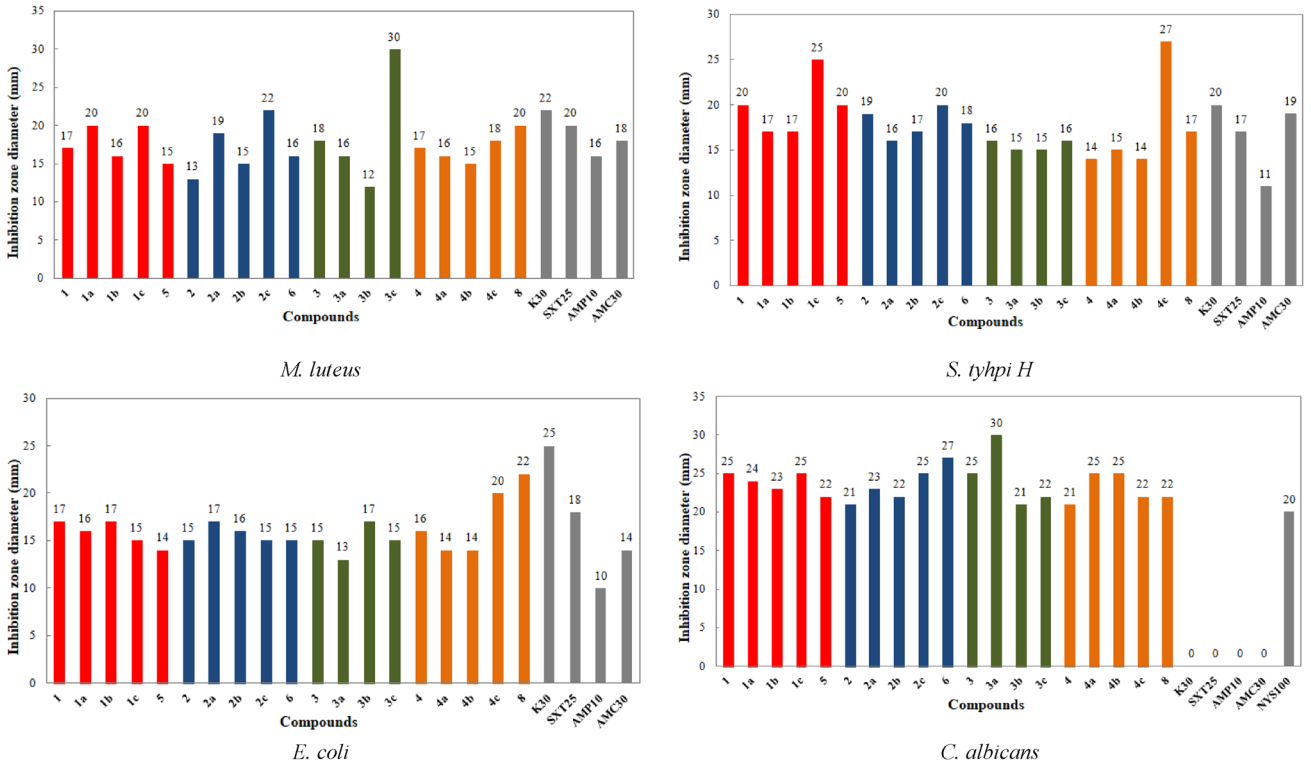

Fig. 3 Antimicrobial activity of synthesized compounds and standard reagents (inhibition zone diameter: mm)

opportunistic pathogen and is associated with food-borne diseases [39, 40].

(iii) Compounds **1, 2b** and **4c** showed high antimicrobial activity in *S. aureus* while compounds **1c, 5, 4, 4a** and **8** showed high activities against *S. epidermidis* (Fig. 2).

(iv) Compounds **1a, 1c, 2a, 2c, 3c** and **8** showed high inhibitory activity against Gram-positive *M.luteus* (Fig. S20). Compound **3c** showed the same inhibitory effect standart AMP10 (25 mm) and AMC30 (24 mm) while showed a greater inhibitory effect than reference drug K30 (25 mm) and SXT25 (24 mm) (Fig. 3).

(v) Compounds **4c** and **8** showed higher inhibitory activity against Gram negative *E. coli*. Furthermore compounds **4c** and **8** showed a greater inhibitory effect than reference drug AMP10 (10 mm), AMC30 (14) and SXT25 (18 mm) (Fig. 3).

(vi) All of compounds showed higher inhibitory activity (20–25 mm) in *S. marcescens* (Fig. S21).

(vii) Compounds 1, **1b, 2a, 3,** and **3a** showed high inhibitory activity against Gram negative *Sh. dys*.

(viii) All of compounds showed higher activity (with zone values of 21–30 mm) in *C.albicans* than the commercial antifungal standard (positive control NYS100P) and compounds **3a** showed the highest activity (30 mm) (Fig. 3) (Fig. S22). For immunocompromised patients (organ or ligament transplantation, cancer chemotherapy, adjuvants) systemic fungal infections (including *C. albicans*) can cause significant mortality and morbidity. [41, 42].

From the result obtained, it is concluded that all of compounds were more effective in Gram (–) bacteria than Gram (+) bacteria (Table 7) (Figs. 2 and 3). The possible reason for this may be the presence of external impermeable membrane, fine peptidoglycan monolayer, presence of periplasmic cavity and cell wall the composition in Gram-negative bacteria [43].

Thermal study

The pyridine rings of ligands **1–4** contain nitro groups. In general, the synthesized compounds in this study are relatively large and have high melting points. After their melting point, an exothermically decomposition reaction took place in the part where the nitro groups were located as expected. However, for the synthesized compounds, it was observed that the exothermic decomposition did not spread to the whole molecule, but occurred locally due to the low number of nitro groups compared to the molecular size (Fig. 4).

Table 7 Antimicrobial activity of new compounds (**1–6**, **8**; **1a–4a**; **1b–4b**; **1c–4c**) and standard reagents

Compound Name	Gram positive bacteria			Gram negative bacteria								Yeast
	L.monocytogenes	*S.typhi H*	*B.cereus*	*S.aureus*	*S.epidermis*	*M.luteus*	*E.coli*	*Klebsiella pneumonia*	*Proteus vulgaris*	*Serratia marcescens*	*Sh. dys*	*C. albicans*
1	–	**20 H**	14 I	**20 H**	17 I	17 I	17 I	–	11 L	**25 H**	**20 H**	**25 H**
1a	–	17 I	15 I	–	18 I	**20 H**	16 I	–	11 L	**21 H**	–	**24 H**
1b	–	17 I	15 I	–	18 I	16 I	17 I	–	11 L	**22 H**	**20 H**	**23 H**
1c	–	**25 H**	17 I	–	**20 H**	**20 H**	15 I	–	–	**22 H**	–	**25 H**
5	15 I	**20 H**	16 I	–	19 I	15 I	14 I	–	11 L	**25 H**	–	**22 H**
2	**20 H**	19 I	18 I	–	17 I	13 L	15 I	12 L	–	**20 H**	–	**21 H**
2a	–	16 I	17 I	–	15 I	19 I	17 I	–	–	**20 H**	**22 H**	**23 H**
2b	–	17 I	12 L	**22 H**	17 I	15 I	16 I	–	11 L	**20 H**	–	**22 H**
2c	14 I	**20 H**	18 I	11 L	16 I	**22 H**	15 I	15 I	13 L	**22 H**	15 I	**25 H**
6	–	18 I	17 I	–	15 I	16 I	15 I	–	12 L	**25 H**	–	**27 H**
3	–	16 I	13 L	–	15 I	18 I	15 I	–	–	**20 H**	**20 H**	**25 H**
3a	–	15 I	13 L	13 L	18 I	16 I	13 I	–	11 L	**22 H**	**25 H**	**30 H**
3b	–	15 I	**20 H**	–	17 I	12 L	17 I	–	11 L	**20 H**	–	**21 H**
3c	17 I	16 I	**20 H**	–	16 I	**30 H**	15 I	15 I	12 L	**22 H**	17 I	**22 H**
4	–	14 I	15 I	13 L	**20 H**	17 I	16 I	–	–	**25 H**	15 I	**21 H**
4a	17 I	15 I	16 I	–	**23 H**	16 I	14 I	–	–	**22 H**	–	**25 H**
4b	**20 H**	14 I	15 I	–	18 I	15 I	14 I	–	11 L	**20 H**	–	**25 H**
4c	**20 H**	**27 H**	16 I	**20 H**	15 I	18 I	**20 H**	12 L	15 I	**20 H**	15 I	**22 H**
8	–	17 I	18 I	–	**22 H**	**20 H**	**22 H**	–	13 L	**25 H**	–	**22 H**
Standards												
K30		20		25			25					–
SXT25		17		24			18					–
AMP10		11		30			10					–
AMC30		19		30			14					–
NYS100		–		–			–					20

H High, *I* Intermediate, *L* Low activity

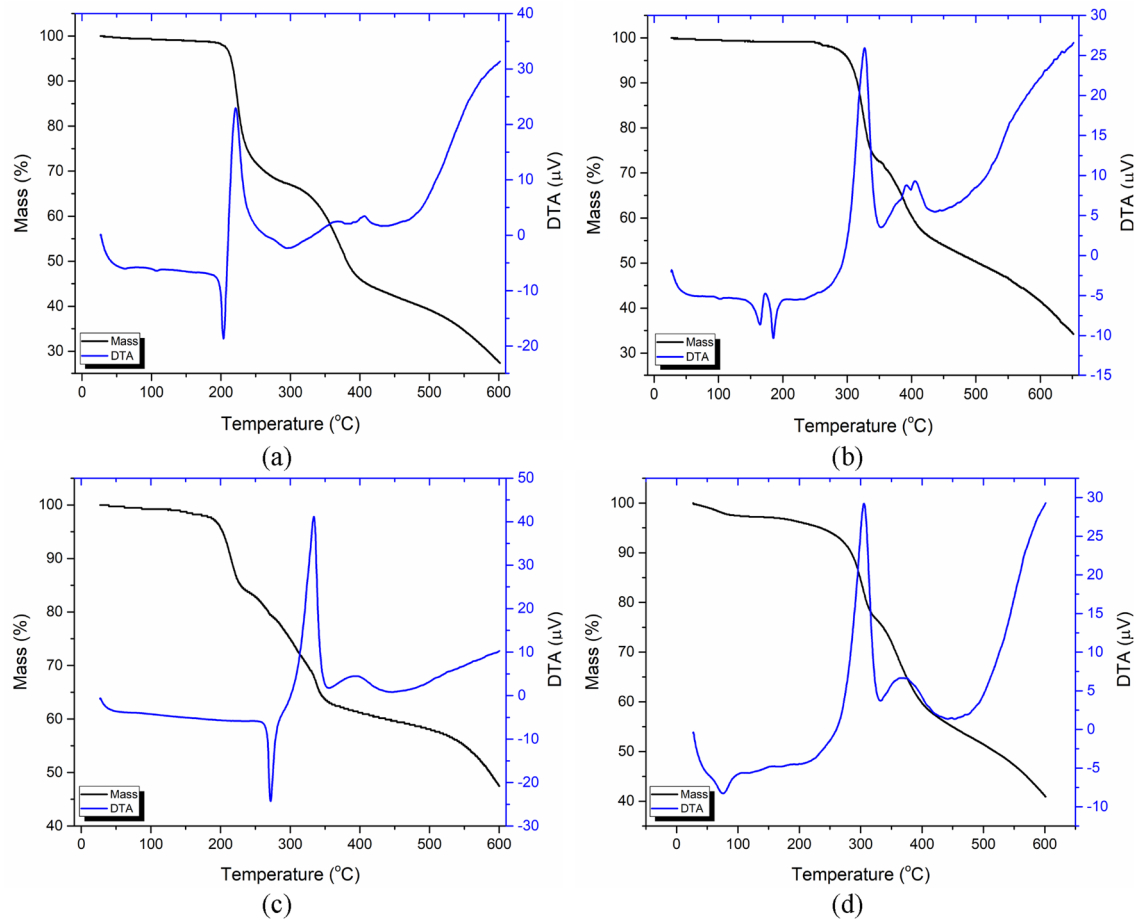

Fig. 4 Thermal behaviors of sythesized ligands **a 1**, **b 2**, **c 3** and **d 4**

Therefore, oxygen balance (Ω) rules are not valid for synthesized compounds [44, 45].

After this degradation in the TG study, the residue continued to decompose as pyrolysis in an inert atmosphere. The mass loss in the molecule was approximately 25% with the exothermic decomposition of nitro groups. As expected, this exothermic degradation was not observed after nitro groups were reduced to amino groups (**5**, **6** and **8**) (Fig. 5).

In the $AgNO_3$ complexes (**1c–4c**) of ligands **1–4**, nitro groups in the pyridine rings and nitrate groups coordinated to the structure or nitrate groups in the structure as neutralizing anions caused exothermic decomposition. However, the exothermic decomposition of nitro and nitrate groups proceeds as a two-step reaction. (Fig. 6). The most important thing observed in the TG curves of the compounds was the steric effect on the nitro groups. Considering the possible structures, the steric effect was found to be **3** < **4** < **2** < **1** from weak to strong. The nitro groups in ligand **3**, which are in the para position, have the least steric effect. They are more free and more open to intermolecular interactions than nitro groups in other ligands. Therefore, the energy released in exothermic decomposition was determined to be inversely proportional to the steric effect. It was observed that the $AgNO_3$ complex (**3c**) of ligand **3** which had a low steric effect, was decomposed by an explosive substance-like exothermic reaction. The mass loss in these fragments also increased inversely proportional with the steric effect [46, 47].

As can be seen in the DTA-Temperature–Time graph, during the explosion of the 3c complex, while the temperature first tended to increase, it shifted to a decreasing direction by making a maximum, and then the temperature increased again in parallel with the furnace temperature (Fig. 7). This phenomenon, which is typically observed in explosion reactions, can be thought of as a result of the gases released during the explosion being removed from the environment by absorbing the explosion heat. The released gases also absorbed some of the pan's and detector's heat. For this reason, the detector temperature remained below the furnace temperature for a short time, then reached the furnace temperature again.

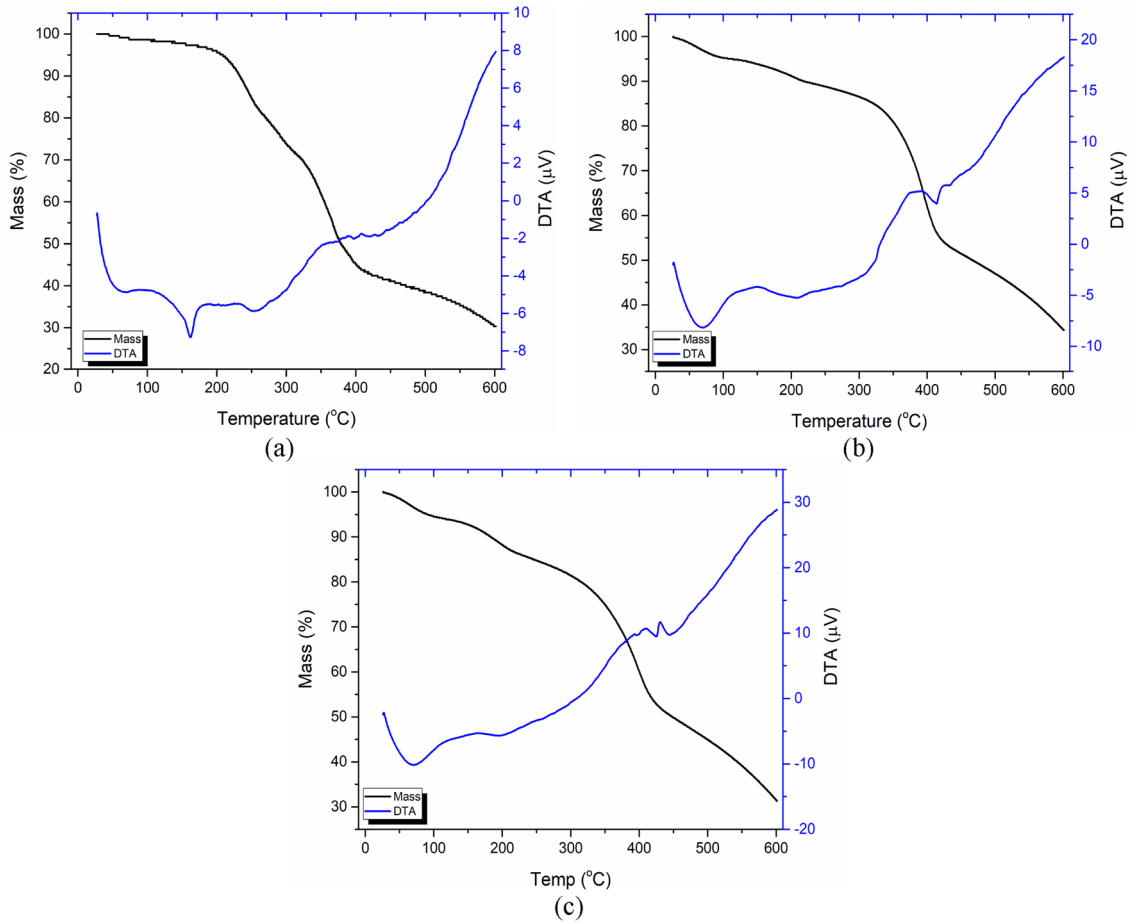

Fig. 5 Thermal behaviors of sythesized amine compounds **a 5**, **b 6** and **c 8**

Figure 8 shows that the TG curve of complex **1c** recorded in O_2 atmosphere. At 600 °C, the amount of residue is around 15%, and the expected residue amount from this complex in an O_2 atmosphere is about 16%. Considering that the organic part is completely converted to CO_2, NO and H_2O compounds in O_2 environment and the residue is Ag_2O, it can be thought that the TG results also confirm the complex stoichiometry.

Conclusions

In this work, double-armed ligands (**1–4**) were synthesized by the reaction of 4′,5′-bis(bromomethyl)benzo-15-crown-5' and substituted pyridine derivatives in basic medium. In addition, amine substituted double-armed crown ether ligands (**5**, **6** and **8**) were obtained by the reduction of compounds **1**, **2** and **4**. Alkali metal (Na^+ and K^+) and transition metal (Ag^+) complexes (**1a–4a**, **1b–4b** and **1c–4c**) of compounds **1–4** were obtained. As expected, it was determined that the sodium ion complexed with the ligand as 1:1 (metal:ligand) and the potassium ion complexed with the ligand as 1:2 (metal:ligand). It was determined that in Ag^+ complexes **1c**, **2c** and **4c**, silver is bi-coordinated, in compound **3c** it is four-coordinated, and the nitrate anion binds to the structure as a bidentate ligand.

The synthesized compounds (**1a–4a**, **1b–4b**, and **1c–4c**) were found to exhibit in general moderate to good antibacterial and antifungal activities for all pathogenic strains used in the study. There have been findings for the compounds that were obtained that could compete with, or even outperform, commercial antibiotics used in the treatment of microbial infections. Consequently is believed that the compounds (specially Ag complexes **1c**, **2c**, **4c**) could be used as an excellent antimicrobial agent against pathogenic microorganisms or as an additive to antimicrobial products.

It has been observed that thermal studies of synthesized ligands (**1–4**), compounds obtained by reduction of those ligands (**5**, **6**, **8**) and silver complexes (**1c–4c**) reveal sufficient findings to confirm the structures and observe

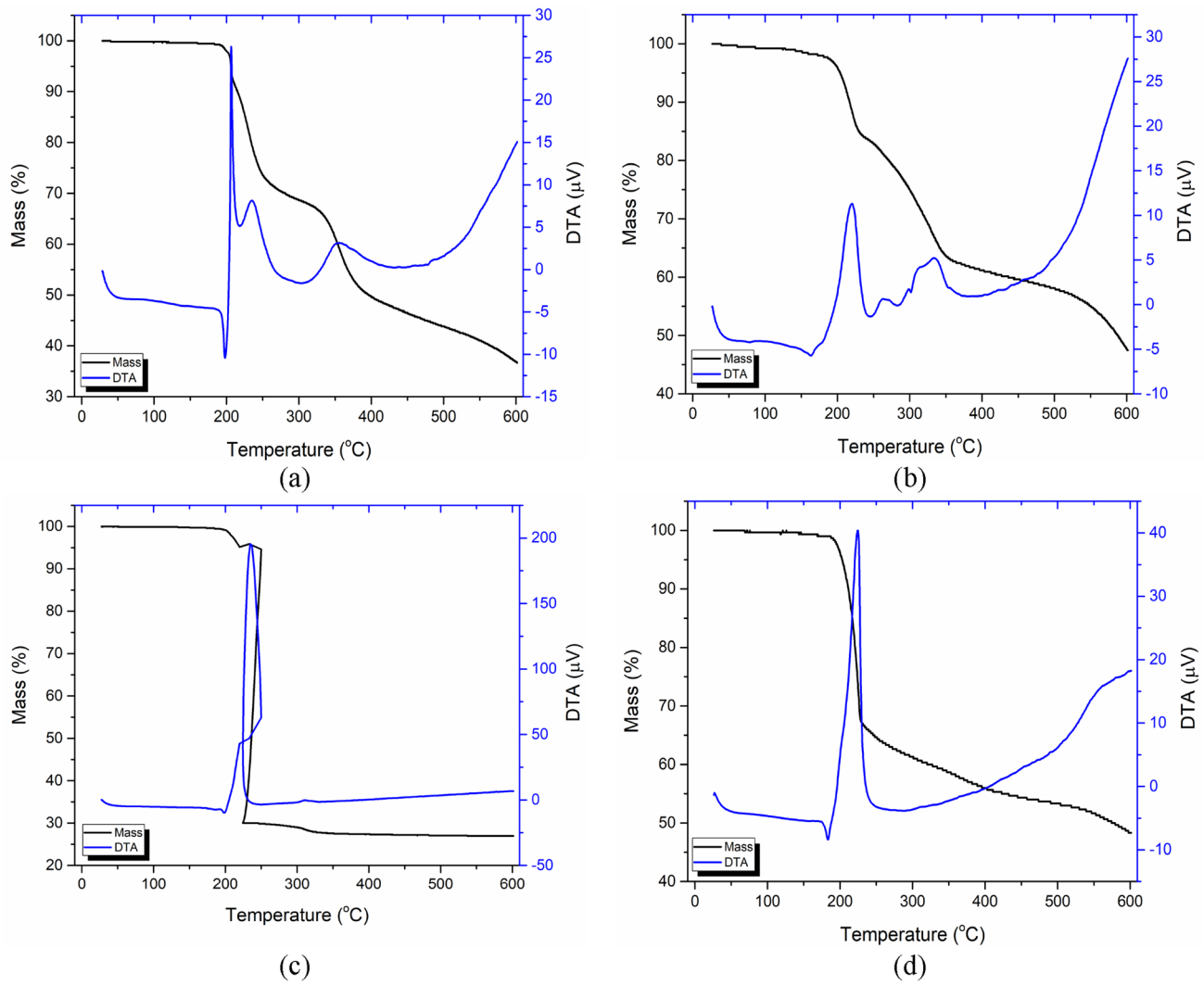

Fig. 6 Thermal behaviors of sythesized Ag^+ complexes **a 1c**, **b 2c**, **c 3c** and **d 4c**

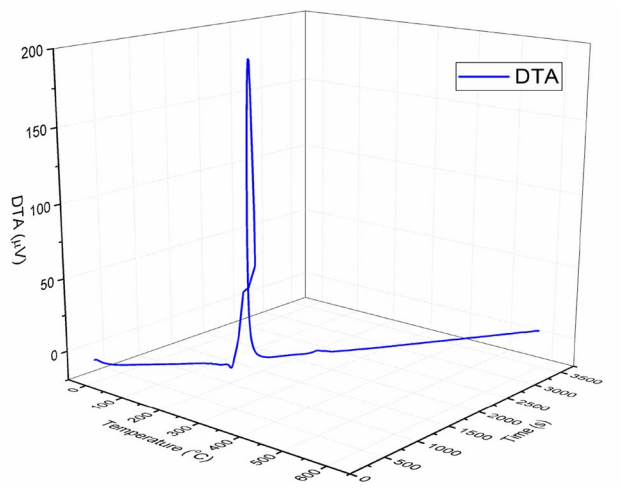

Fig. 7 DTA-Temperature–Time graphic for compound **3c**

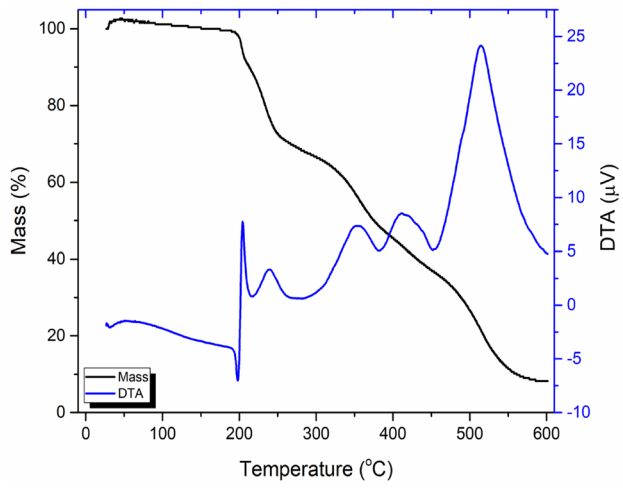

Fig. 8 Thermal behaviors of sythesized Ag^+ complex **1c** in O_2 atmosphere

the thermal properties. In the study, besides observing the characteristic thermal behaviors of nitro groups, amine groups obtained by reduction of nitro groups and complexes synthesized with silver nitrate, it was determined in accordance with the literature that the positions of nitro groups in the compounds are important in terms of structural characteristics.

Supplementary Information The online version contains supplementary material available at https://doi.org/10.1007/s10847-022-01157-y.

Acknowledgements The authors gratefully acknowledge the financial assistance of the Scientific and Technical Research Council of Turkey (TUBITAK), Grant No: TBAG 210T122, and Ankara University Grant No: 17B0430004.

Declarations

Conflict of interest The authors declare no confict of interest.

References

1. Pedersen, C.J.: Cyclic polyethers and their complexes with metal salts. J. Am. Chem. Soc. **89**, 7017–7036 (1967). https://doi.org/10.1021/ja01002a035
2. Pedersen, C.J.: The discovery of crown ethers. Science **241**, 536–540 (1988). https://doi.org/10.1126/science.241.4865.536
3. Gokel, G.W., Leevy, W.M., Weber, M.E.: Crown ethers: sensors for ions and molecular scaffolds for materials and biological models. Chem. Rev. **104**, 2723–2750 (2004). https://doi.org/10.1021/cr020080k
4. Li, J., Yim, D., Jang, W.D., Yoon, J.: Recent progress in the design and applications of fluorescence probes containing crown ethers. Chem. Soc. Rev. **46**, 2437–2458 (2017). https://doi.org/10.1039/C6CS00619A
5. Zhang, G., Zhang, D., Zhou, Y., Zhu, D.: A new tetrathiafulvalene-anthracence dyad fusion with the crown ether group: fluorescence modulation with Na^+ and C^{60}, mimicking the performance of an "AND" logic gate. J. Org. Chem. **71**, 3970–3972 (2006). https://doi.org/10.1021/jo052494u
6. Gawley, R.E., Mao, H., Haque, M.M., Thorne, J.B., Pharr, J.S.: Visible fluorescence chemosensor for saxitoxin. J. Org. Chem. **72**, 2187–2191 (2007). https://doi.org/10.1021/jo062506r
7. Pond, S.J.K., Tsutsumi, O., Rumi, M., Kwon, O., Zojer, E., Brédas, J.L., Marder, S.R., Perry, J.W.: Metal-ion sensing fluorophores with large two-photon absorption cross sections: Aza-crown ether substituted donor-acceptor-donor distyrylbenzenes. J. Am. Chem. Soc. **126**, 9291–9306 (2004). https://doi.org/10.1021/ja049013t
8. Tso, W.W., Fung, W.P.: Correlation between the antibacterial activity and alkali metal ion transport efficiency of crown ether. Inorg. Chim. Acta **55**, 129–134 (1981). https://doi.org/10.1016/S0020-1693(00)90794-1
9. Marjanović, M., Kralj, M., Supak, F., Frkanec, L., Piantanida, I., Šmuc, T., Tušek-Božić, L.: Antitumor potential of crown ethers: structure-activity relationships, cell cycle disturbances, and cell death studies of a series of ionophores. J. Med. Chem. **50**, 1007–1018 (2007). https://doi.org/10.1021/jm061162u
10. Altaf, M., Stoeckli-Evans, H., Cuin, A., Sato, D., Pavan, F., Leite, C., Ahmad, S., Bouakka, M., Mimouni, M., Khardli, F., Hadda, T.: Synthesis, crystal structures, antimicrobial, antifungal andantituberculosis activities of mixed ligand silver(I) complexes. Polyhedron **138**, 138–147 (2013). https://doi.org/10.1016/j.poly.2013.06.021
11. Koçoğlu, S., Hayvali, Z., Ogutcu, H.: A polydentate ligand based on 2,2'-dipyridylamine unit linked benzo-15-crown-5; alkali and transition metal complexes; photoresponsive ligand; antimicrobial evaluation against pathogenic microorganisms. Trans. Met. Chem. **46**, 509–522 (2021). https://doi.org/10.1007/s11243-021-00469-1
12. Hayvalı, Z., Guler, H., Ogutcu, H., Sarı, N.: Novel bis-crown ethers and their sodium complexes as antimicrobial agent: synthesis and spectroscopic characterizations. Med. Chem. Res. **23**, 652–3661 (2014). https://doi.org/10.1007/s00044-014-0937-9
13. Ackermann, L., Diers, E., Manvar, A.: Ruthenium-catalyzed C−H bond arylations of arenes bearing removable directing groups via six-Mmembered ruthenacycles. Org. Lett. **14**, 1154–1157 (2012). https://doi.org/10.1021/ol3000876
14. Liang, Y.F., Li, X., Wang, X., Yan, Y., Feng, P., Jiao, N.: Aerobic oxidation of PdII to PdIV by active radical reactants: direct C−H nitration and acylation of arenes via oxygenation process with molecular oxygen. ACS Catal. **5**, 1956–1963 (2015). https://doi.org/10.1021/cs502126n
15. Lou, S.J., Chen, Q., Wang, Y.F., Xu, D.Q., Du, X.H., He, J.Q., Mao, Y.J., Xu, Z.Y.: Selective C-H bond fluorination of phenols with a removable directing group: late-stage fluorination of 2-phenoxyl nicotinate derivatives. ACS Catal. **5**, 2846–2849 (2015). https://doi.org/10.1021/acscatal.5b00306
16. Dai, W.C., Yang, B., Xu, S.H., Wang, Z.X.: Nickel-catalyzed cross-coupling of aryl 2-pyridyl ethers with organozinc reagents: removal of the directing group via cleavage of the carbon-oxygen bonds. J. Org. Chem. **86**, 2235–2243 (2021). https://doi.org/10.1021/acs.joc.0c02389
17. Fleming, G.J.: Thermal analysis of nitro-substituted epoxide polymers. J. App. Polym. Sci. **13**, 2579–2592 (1969). https://doi.org/10.1002/app.1969.070131206
18. Yigiter, A.O., Atakol, M.K., Aksu, M.L., Atakol, O.: Thermal characterization and theoretical and experimental comparison of picryl chloride derivatives of heterocyclic energetic compounds. J. Therm. Anal. Calorim. **127**, 2199–2213 (2017). https://doi.org/10.1007/s10973-016-5766-2
19. Bernt, S., Guillerm, V., Serre, C., Stock, N.: Direct covalent post-synthetic chemical modification of Cr-MIL-101 using nitrating acid. Chem. Commun. **47**, 2838–2840 (2011). https://doi.org/10.1039/C0CC04526H
20. Atakol, A., Svoboda, I., Dal, H., Atakol, O., Nazır, H.: New energetic silver(I) complexes with Nnn type pyrazolylpyridine ligands and oxidizing anions. J. Mol. Struct. **1210**, 128001 (2020). https://doi.org/10.1016/j.molstruc.2020.128001
21. Bilgin, A., Ertem, B., Dinc Agın, P., Gok, Y., Karslıoglu, S.: Synthesis, characterization and extraction studies of a new vic-dioxime and its complexes containing bis(diazacrown ether) moieties. Polyhedron **25**, 3165–3172 (2006). https://doi.org/10.1016/j.poly.2006.05.023
22. Koçoğlu, S., Ogutcu, H., Hayvalı, Z.: Photophysical and antimicrobial properties of new double-armed benzo-15-crown-5 ligands and complexes. Res. Chem. Intermed. **45**, 2403–2427 (2019). https://doi.org/10.1007/s11164-019-03741-3
23. Calverley, M.J., Dale, J.: 1,4,7-Trioxa-10-azacyclododecane and some N-substituted derivatives; Synthesis and cation complexing. Acta Chem. Scand. B. **36**, 241–247 (1982). https://doi.org/10.3891/acta.chem.scand.36b-0241
24. Winkler, B., Mau, A.W.H., Dai, L.: Crown ether substituted phenylenevinylene oligomers: synthesis and electroluminescent properties. Phys. Chem. Chem. Phys. **2**, 291–295 (2000). https://doi.org/10.1039/A907547J
25. Sarı, N., Şahin, S.Ç., Öğütcü, H., Dede, Y., Yalçın, S., Altundas, A., Doğanay, K.: Ni(II)-tetrahedral complexes: characterization,

antimicrobial properties, theoretical studies and a new family of charge-transfer transitions. Spectrochim. Acta A. **106**, 60–67 (2013). https://doi.org/10.1016/j.saa.2012.12.078
26. Rubab, S., Bahadur, S., Hanif, U., Durrani, A.I., Sadiqa, A., Shafique, S., Zafar, U., Shuaib, M., Urooj, Z., Nizamani, M.M., Iqbal, S.: Phytochemical and antimicrobial investigation of methanolic extract/ fraction of *Ocimum basilicum* L. Biocatal. Agric. Biotechnol. **31**, 101894 (2021). https://doi.org/10.1016/j.bcab.2020.101894
27. Nartop, D., Sarı, N., Altundaş, A., Öğütcü, H.: Synthesis, characterization, and antimicrobial properties of new polystyrene-bound Schiff bases and their some complexes. J. Appl. Polym. Sci. **125**, 1796–1803 (2012). https://doi.org/10.1002/app.36270
28. Çınarlı, M., Yüksektepe Ataol, Ç., Bati, H., Güntepe, F., Ögütçü, H., Büyükgüngör, O.: Synthesis, structural characterization, Hirshfeld analyses, and biological activity studies of Ni(II) and Zn(II) complexes containing the sulfonohydrazone group. Inorg. Chim. Acta **484**, 87–94 (2019). https://doi.org/10.1016/j.ica.2018.09.027
29. Barboiu, M., Meffre, A., Legrand, Y.M., Petit, E., Marin, L., Pinteala, M., Lee, A.V.D.: Frustrated ion-pair binding by heteroditopic macrocyclic receptors. Supramol. Chem. **26**, 223–228 (2014). https://doi.org/10.1080/10610278.2013.852196
30. Poonia, N.S., Bagdi, P., Sidhu, K.S.: Structural aspects of crown complexes with alkali and alkaline earth cations. Benzo-15-crown-5 as a discriminating macrocycle. J. Incl. Phenom. **4**, 43–54 (1986). https://doi.org/10.1007/BF00662080
31. Keller, B.O., Sui, J., Young, A.B., Whittal, R.M.: Interferences and contaminants encountered in modern mass spectrometry. Anal. Chim. Acta **627**, 71–81 (2008). https://doi.org/10.1016/j.aca.2008.04.043
32. Tong, H., Bell, D., Tabei, K.: Siegel, MM: Automated data massaging, interpretation, and e-mailing modules for high throughput open access mass spectrometry. J. Am. Soc. Mass. Spectrom. **10**, 1174–1187 (1999). https://doi.org/10.1016/S1044-0305(99)00090-2
33. Ghildiyal, N., nee Pant, G.J., Rawat, M.S.M., Singh, K.: Spectral investigation of the effect of anion on the stability of non covalent assemblies of 2,3,5,6,8,9,11,12-octahydro-1,4,7,10,13-benzopentaoxacyclopentadecine (benzo-15-crown-5) with sodium halides. Spectrochim. Acta A. **171**, 507–514 (2017). https://doi.org/10.1016/j.saa.2016.07.044
34. Liu, Y.: Han, JR, Zhang, HY: Assembly behavior and binding ability of double-armed benzo-15-crown-5 with the potassium ion. Supramol. Chem. **16**, 247–254 (2004). https://doi.org/10.1080/10610270410001663796
35. Şahin, D., Süzen, Y., Hayvalı, Z.: Double-armed benzo-15-crown-5 ligands and complexes and single crystal structure determination. Heteroatom Chem. **25**, 43–54 (2014). https://doi.org/10.1002/hc.21134
36. Şahin, D., Koçoğlu, S., Şener, O., Şenol, C., Dal, H., Hokelek, T., Hayvalı, Z.: New NO donor ligands and complexes containing furfuryl or crown ether moiety: Syntheses, crystal structures and tautomerism in ortho-hydroxy substituted compounds as studied by UV-vis spectrophotometry. J. Mol. Struct. **1102**, 302–313 (2015). https://doi.org/10.1016/j.molstruc.2015.09.004
37. Öğütçü, H., Kurnaz Yetim, N., Hasanoglu Özkan, E., Eren, O., Kaya, G., Sarı, N., Dişli, A.: Nanospheres caped Pt(II) and Pt (IV): synthesis and evaluation as antimicrobial and antifungal agent. P. J. Chem. Techn. **19**, 74–80 (2017). https://doi.org/10.1515/pjct-2017-0011
38. Çiçek, İ, Tunç, T., Ogutcu, H., Abdurrahmanoglu, S., Günel, A., Demirel, N.: Synthesis of novel chiral aminoalcohol and benzimidazole hybrids and investigation of their antimicrobial activities. Bioorg. Chem. **5**, 4650–4654 (2020). https://doi.org/10.1002/slct.202000355
39. Gul, D.S., Ogutcu, H., Hayvalı, Z.: Investigation of photophysical behavior and antimicrobial activity of novel benzo-15-crown-5 substituted coumarin and chromone derivatives. J. Mol. Struct. **1204**, 127569 (2020). https://doi.org/10.1016/j.molstruc.2019.127569
40. Nartop, D., Hasanoğlu Özkan, E., Gündem, M., Çeker, S., Ağar, G., Öğütcü, H., Sarı, N.: Synthesis, antimicrobial and antimutagenic effects of novel polymeric-Schiff bases including indol. J. Mol. Struct. **1195**, 877–882 (2019). https://doi.org/10.1016/j.molstruc.2019.06.042
41. Altundas, A., Erdogan, Y., Ögütcü, H., Kizil, H.E., Agar, G.: Synthesis and in-vitro antimicrobial and anti-mutagenic activities of some novel 2-(2-hydroxybenzylideneamino)-5,7-dihydro-4H-thieno[2,3-c]pyran-3-carbonitrile derivatives. Fresen. Environ. Bull. **25**, 5411–5418 (2016)
42. Nartop, D., Demirel, B., Güleç, M., Hasanoğlu Özkan, E., Kurnaz Yetim, N., Sarı, N., Çeker, S., Öğütcü, H., Ağar, G.: Synthesis, enzyme immobilization, antimutagenic activity and antimicrobial evulation against pathogenic microorganisms. J. Biochem. Mol. Tox. **34**, e22432 (2020). https://doi.org/10.1002/jbt.22432
43. Afzal, J., Ullah, N., Hussain, Z., Rukh, S., Ayaz, M., Akbar, A., Zaman, A.: Phytochemical an analysis and antibacterial potential of leaf extract of Bauhinia Linn.: An ethnomedicinal plant. Matrix Science Pharma **1**, 17–19 (2017). https://doi.org/10.26480/msp.02.2017.17.19
44. Atakol, O., Fuess, H., Kurtaran, R., Akay, A., Arici, C., Ergun, Ü.: Emregül, KC: Three new dinuclear silver(I) complexes derived from pyrazolyl type ligands. J. Therm. Anal. Calorim. **90**, 517–523 (2007). https://doi.org/10.1007/s10973-006-7689-9
45. Klapötke, T.M.: Chemistry of high-energy materials, 3rd edn. De Gruyter, Berlin (2015)
46. Lizarraga, E., Zabaleta, C.: Palop, JA: thermal stability and decomposition of pharmaceutical compounds. J. Therm. Anal. Calorim. **89**, 783–792 (2007). https://doi.org/10.1007/s10973-006-7746-4
47. Apreutesei, D., Lisa, G., Hurduc, N., Scutaru, D.: Thermal behavior of some cholesteric esters. J. Therm. Anal. Calorim. **83**, 335–340 (2006). https://doi.org/10.1007/s10973-005-6522-1